
MANY EPISODE LEARNING IN A MODULAR EMBODIED AGENT VIA END-TO-END INTERACTION

Yuxuan Sun Ethan Carlson Rebecca Qian Kavya Srinet Arthur Szlam

Meta AI Research

ABSTRACT

In this work we give a case study of a modular embodied machine-learning (ML) powered agent that improves itself via interactions with crowd-workers. The agent consists of a set of modules, some of which are learned, and others heuristic. While the agent is not “end-to-end” in the ML sense, end-to-end interaction with humans and its environment is a vital part of the agent’s learning mechanism. We describe how the design of the agent works together with the design of multiple annotation interfaces to allow crowd-workers to assign credit to module errors from these end-to-end interactions, and to label data for an individual module. We further show how this whole loop (including model re-training and re-deployment) can be automated. Over multiple loops with crowd-sourced humans with no knowledge of the agent architecture, we demonstrate improvement over the agent’s language understanding and visual perception modules.

1 INTRODUCTION

Present day machine learning (ML) research prioritizes end-to-end learning. Not only are end-to-end models able to achieve excellent performance on static tasks, there is a growing literature on how to adapt pre-trained networks to new tasks, and large pre-trained models can have impressive zero-shot performance on unseen tasks. In the setting of embodied agents, this manifests as agents actualized as monolithic ML models, where inputs to the model are the agent’s perceptual sensors, and the model’s outputs directly control agent actions. There are now a number of environments designed for the training of end-to-end embodied agents [Beattie et al. \(2016\)](#); [Savva et al. \(2019\)](#); [Guss et al. \(2019\)](#); [Petrenko et al. \(2021\)](#), and there is hope (and some evidence) that the same sort of transfer and adaptability seen in language and vision models will carry over to the embodied agent setting.

Nevertheless, agents implemented as fully end-to-end ML models are rare in production systems (or in real-world embodied agents, a.k.a. robots). While this in part is a symptom of the rapid improvement and scaling in the literature and the lag in technology transfer, these systems require performance and safety guarantees that are still not easily obtainable from end-to-end ML models; and must be maintainable by human engineers. On the other hand, it is difficult for pipelined agents to learn from experience once deployed. Instead, human engineers design a module, collect and collate data for it, train the appropriate ML model, and then deploy it. Thus the agent’s abilities don’t scale directly with the experience it receives, but rather with the amount of human engineering power that can be brought to bear in building the modules. To somewhat oversimplify, engineers trade off ML scalability (the ability to learn new things through interaction, without engineering investment) for modularity, serviceability, and interpretability.

This work is a case study of automating self-improvement via interactions with people in a pipelined ML-powered agent. The agent consists of a set of modules, some of which are learned, and others heuristic. The agent is not “end-to-end” in the ML sense, but end-to-end interaction, in the sense of players interacting with the full agent system, is a vital part of the agent’s learning mechanism.

Our main result is demonstrating that subsystems in the agent can be improved with signal from these end-to-end interactions, further augmented with annotation tasks routed from marked errors. The crucial point is that with appropriate UX (user experience) design, sets of crowd-workers with no special training (and in particular, without any knowledge of the agent architecture or any agent modules) are able to assign credit to module errors and annotate them at scale. We fully automate a loop of human-agent interaction, credit-assignment, module-data-annotation, model-retraining and re-deployment, and show that this successfully improves the agent’s neural semantic parsing module (a finetuned BERT encoder with decoder trained from scratch) and visual perception module (a CLIP-style vision model) over multiple iterations. We thus give evidence that it is possible to keep modularity without giving up ML scalability in this setting.

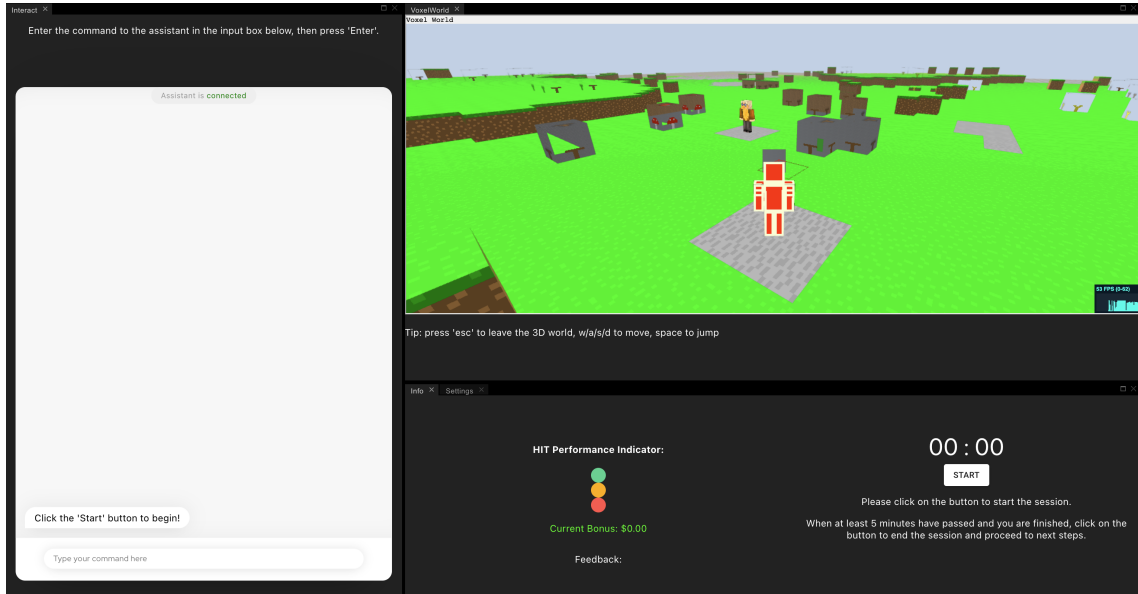


Figure 1: An image of the dashboard user interface seen by crowd workers in production.

2 SETTING AND METHODS

2.1 THE SETTING

We describe the agent architecture and the world in which it lives.

2.1.1 WORLD

The agent is embodied in a three dimensional voxel world. Each voxel can be occupied by space or an impassable block of material. Movement is possible in any direction, as long as the voxel is unoccupied; and the agent moves via discrete steps of size one voxel. The agent also can turn to look in any direction; and so its pose can be represented by a $(x, y, z, \text{pitch}, \text{yaw})$ tuple. In addition to being able to act by changing its body or head position, the agent can point at rectangular regions of space (by visibly flashing them), and can “speak” in text. The agent can also place blocks of various colors, or destroy them.

A human player co-occupies the world with the agent. The human player’s pose is determined by an $(x, y, z, \text{pitch}, \text{yaw})$ tuple. The human player can also speak in text to the agent, and the agent can see the human player’s pose (including the pitch and yaw, allowing it to decide what the human is looking at). The human can place blocks and destroy blocks. See the interface in Figure 1.

2.1.2 THE AGENT

We use a Droidlet agent [Pratik et al. \(2021\)](#). The agent’s perceptual input includes the location of the agent’s self pose, the player’s pose, the location and type (i.e. material) of each block in space, and the chat history. It is equipped with heuristic perceptual methods to recognize connected components of blocks and the local ground plane. It is also equipped with a CLIP-style visual perceptual module which can predict segmentation of objects referred with natural language descriptions. It makes use of a BERT-based semantic parsing model further described in Section 2.3 as its natural language understanding (NLU) “perception”.

The agent has heuristic, scripted “Tasks” that allow execution of atomic programs like movement to locations in space, re-orienting pose, pointing, or placing blocks. The agent has a limited, scripted dialogue capabilities (also implemented as Tasks) to ask clarification questions to the human players when the agent is uncertain about something (for example if the human says “destroy the red cube” and there are two red cubes in the scene, the agent might decide to ask the human which cube they meant, by pointing at one of them).

The parameters of these Tasks are provided by a “Controller” module that inputs a partially specified program in the agent’s domain specific language (DSL), either from the output of the NLU module or from the agent’s intrinsic behaviors, and, using the agent’s memory system, fully specifies the program. See [Pratik et al. \(2021\)](#) for more details

2.2 NLU DETAILS

The agent uses a neural semantic parser (NSP) to convert commands from players into partially specified programs in the agent’s DSL; these are fully specified into executable Tasks in the agent’s interpreter, see [Pratik et al. \(2021\)](#) for details. The neural semantic parser is one of the two ML module that has been shown to improve over the course of our experiments in this paper.

The agent’s DSL is similar to the one described in [Srinet et al. \(2020\)](#), using the same top-level commands (Move/Dance, Build/Copy/Destroy/Dig, Stop/Resume), but the children of these have been expanded. For example, a “Copy” top-level command might take a “ReferenceObject” (corresponding to some object in the world) as a child, and the possible queries to specify that ReferenceObject have been expanded from [Srinet et al. \(2020\)](#). The full grammar is included in the supplemental, and some examples are displayed in [Figure 2](#).

The architecture of agent’s semantic parsing model is similar to the one described in [Srinet et al. \(2020\)](#). It is an encoder-decoder seq2seq model where the encoder is finetuned from BERT [Devlin et al. \(2019\)](#) using [hug](#), and the decoder is trained from scratch. In order to use a sequence based decoder, we linearize the target logical forms in depth-first order.

2.3 VISION MODULE DETAILS

The agent uses a 3D referring object segmentation model to detect objects specified by ungrounded natural language expressions. The vision module takes in the 3D voxel world state, as well as text-based “ReferenceObject” descriptions extracted from DSL of NLU outputs and output 3D segmentation masks. The vision model is the second ML module that has been shown to improve over the course of our experiments in this paper.

The architecture of agent’s vision model is similar to [Radford et al. \(2021\)](#), but in a 3D setting. It consists of a Voxel Encoder which is 4-layer convolutional neural network trained from scratch, a Text Encoder which we directly took from CLIP [Radford et al. \(2021\)](#). The output of the model is the probability of being classified as the referred object on each voxel. All voxels with probability high than a threshold are then used to construct the segmentation mask. See more details of model architecture in [Appendix B](#).

The initial dataset used to train the baseline vision model is generated using rule-based scripts. More specifically, we construct schematics of various shape objects using mathematical formulas in a flat 3D voxel world described in [2.1.1](#). Full details and some examples are included in [Appendix B](#).

2.4 LEARNING FROM HUMANS

Human workers are connected with an agent online. They interact with it through their web browser, where we render the agent and a representation of the world. Interaction data is gathered through crowd-sourced tasks where the workers are instructed to issue free form commands to the agents, using a category of actions from a suggested list of agent’s capabilities (eg. ‘build’, ‘destroy’). The workers are given no other instructions about what type of commands to give, other than to be creative and diverse.

After each command, workers are prompted as to whether the task was carried out correctly end-to-end, whether the command was correctly understood, and whether the agent correctly perceived the objects that the workers referred to. If the player marks that the command was not correctly understood, then this command and the agent’s parse are recorded as an NLU error. If the player marks that the agent did not correctly perceived the objects that the workers referred to, then this command, along with a snapshot of the world state, are recorded as a vision error.

These marked NLU errors are then routed to *another* set of qualified crowd workers who write the ground truth parses for these commands. These parse annotation tasks are further distributed into small tasks consisting of 1-3 questions that determine the annotation of a particular node in the parse tree. These full annotations are then used as training data to improve the NLU model offline. The same applies to the vision errors where they are routed to a vision annotation tool for annotation, and then used as training data to improve vision models offline. These retrained models are then re-deployed before the next set of human interactions with the agent. [Figure 3](#) has a diagram showing the agent learning pipeline. The entire pipeline operates autonomously, from launching interaction jobs, to error annotation, to model retraining, to re-deployment.

```

"dig a moat around the fort":
{
  "action_sequence": [
    {
      "action_type": "DIG",
      "location": {
        "relative_direction": "AROUND",
        "reference_object": {
          "filters": {
            "where_clause": {
              "AND": [{"pred_text": "has_name",
                "obj_text": [0, [5, 5]]}]
            }
          }
        }
      }
    }
  ],
  "schematic": {
    "filters": {
      "where_clause": {
        "AND": [{"pred_text": "has_name",
          "obj_text": [0, [2, 2]]}]
      }
    }
  }
}
}

"move to the left of the cube":
{
  "action_sequence": [
    {
      "action_type": "MOVE",
      "location": {
        "relative_direction": "LEFT",
        "reference_object": {
          "filters": {
            "where_clause": {
              "AND": [{"pred_text": "has_name",
                "obj_text": [0, [6, 6]]}]
            }
          }
        }
      }
    }
  ]
}

"build a box":
{
  "action_sequence": [
    {
      "action_type": "BUILD",
      "schematic": {
        "filters": {
          "where_clause": {
            "AND": [{"pred_text": "has_name",
              "obj_text": [0, [2, 2]]}]
          }
        }
      }
    }
  ]
}

```

Figure 2: Some examples of commands that can be parsed in the agent’s DSL. Fields of the form $[x, [y, z]]$ where x , y , and z are numbers are *spans* of text (e.g. the y through z th tokens on the x th text input). Fields with keys “filters” correspond to queries to the agent’s database.

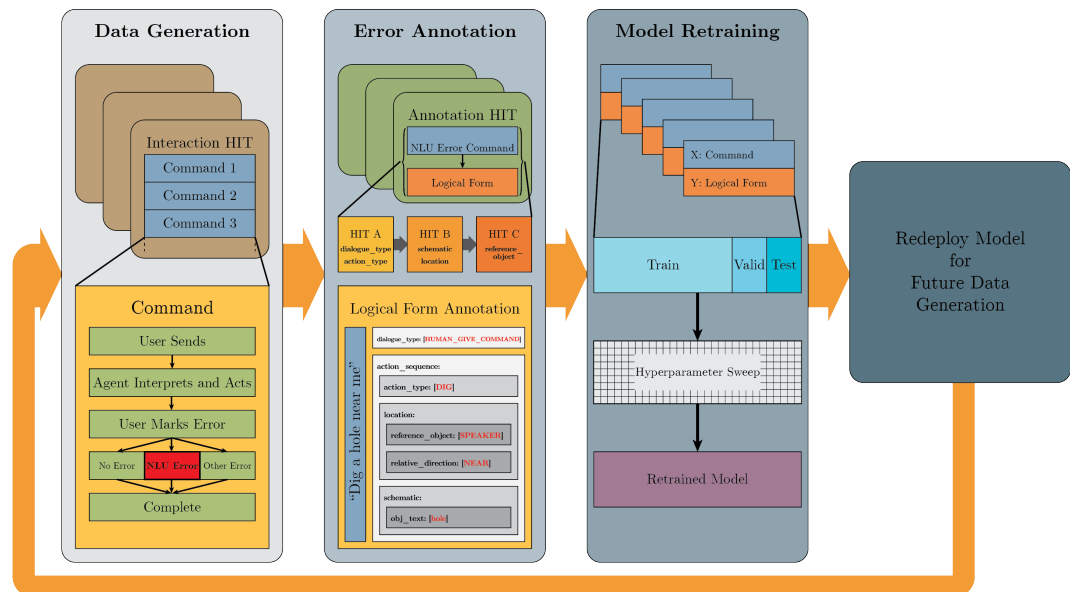


Figure 3: A diagram showing the Droidlet agent’s NLU module improvement with crowd-worker interactions. Note that the workers have no knowledge of the agent architecture. The logical form above has been simplified for clarity.

2.4.1 CHALLENGES OF CROWD-SOURCING HUMAN-AGENT INTERACTIONS

Working with humans in the loop involves challenges that go beyond model architectures and learning algorithms. Apart from making tools that are effective for cooperative people, it is necessary to plan for annotators that will sometimes behave erratically, or even adversarially.

A major issue (common to many crowd-worker deployments) has been - dealing with workers who, covertly or overtly, try to cheat their way through the task. Cheating in this case could mean not doing the task at all, trying to game our qualification criteria, or simply doing the bare minimum to pass but not engaging with the task. The combination of the following methods has allowed for very high quality data collection:

- Workers must first qualify for our interaction task by answering a simple set of questions to prove they are not a bot and are capable of reading the instructions.
- We disable the submission button until a basic list of criteria have been met, and we don't advertise what those criteria are beyond the task instructions.
- By offering performance incentives, we make it more profitable to not cheat than to cheat.
- We blacklist workers who repeatedly perform poorly.
- We ask workers to reflect on their own performance, which facilitates perspective-taking and improved performance on repeated iterations of the task. [Dow et al. \(2012\)](#)

Even workers who are not acting adversarially can present challenges to development. They may not understand the instructions if not presented clearly, their knowledge of the English language may vary, and they may not have a strong aptitude with technology to navigate the interface. These constraints necessitate a focus on usability and user testing throughout the life cycle of the project.

While the human factor presents varied challenges to the development of the agent interface, it has also created a continuous feedback cycle that facilitates overall agent improvement. We have many users of the system issuing thousands of commands, some of which cause the agent to crash or behave in unexpected ways. We would not discover these edge cases very quickly on our own.

2.4.2 ERROR ROUTING

There could be several types of issues that cause the agent to fail to execute a command. One example is that the user asks the agent to do something that is not expressible in its DSL ("let's play chess") or that is in its DSL, but part of the command refers to something the agent does not know ("build a camel" and the agent does not know what a "camel" is). The agent can also fail because its visual perception module did not recognize an object, because it did not correctly retrieve the right information from memory, and the focus of this paper: because the NLU model failed to accurately parse the command.

Differentiating between these types of failure is essential for being able to route the correct data to the correct annotator. In the current operation, only commands that are marked as containing an NLU error are sent to be annotated so that ground truth for those commands is added to the training dataset.

This process of differentiating between types of errors is executed using a decision tree that is presented to the worker one question at a time. In the Appendix there are examples of this decision tree in [Figure 17](#), which represents the correct error marking flow after an NLU error, and [Figure 18](#), which represents the error marking flow after a non-NLU task error.

3 RELATED WORK

There is a large literature on human in the loop machine learning, see [Wu et al. \(2021\)](#) for a survey.

Our setting is an embodied agent with a language interface. There is existing work showing improvement after multiple rounds of re-deployment with dialogue agents, for example [Hancock et al. \(2019\)](#); [Shuster et al. \(2021\)](#); [Kiela et al. \(2021\)](#).

Some prior work building towards sophisticated interactive tools for "machine teaching" [Simard et al. \(2017\)](#), where ML naive users are able to guide model training towards high accuracy and coverage, has been considered in the literature and many such tools exist as deployed services, for example [Ratner et al. \(2017\)](#) (commercialized at <https://snorkel.ai/>) or <https://scale.com/>. These are superior to the re-deployment loop described in this work in the sense that the model re-training occurs "in-session", and the machine teacher can immediately see the results of their annotations and adjust accordingly. Furthermore, these also have tools for automatically generating labeled data from rules or automating data augmentation. However, the work described in this case study is complementary to these, in that it focuses on automating the end-to-end data-collection and retraining of ML models that are important internal components of an embodied agent. We give evidence that fully modular ML systems will be able to

self-improve even if gradients cannot pass from one part of the system to another. In future work, we hope to combine our system with responsive in-session learning as described in these services.

Our work is inspired by Wang et al. (2017), where multiple rounds of users build up a semantic parser for a voxel world editor. In Shah et al. (2021) the authors propose a competition to train embodied agents in a voxel world through language descriptions. Our work is also related to Suhr et al. (2019), where the authors build an interactive environment where (embodied) players and agents (playing as the role of a language issuing “leader” with full observability or faster moving “follower” with partial observability) collaborate via natural language to collect cards by moving to their spatial locations. A followup Kojima et al. (2021) is especially relevant; in that work they show how multiple rounds of learning can continue to improve the language generation capabilities of a “leader” model. In addition to the embodied agents and players, our work shares with Kojima et al. (2021) multiple rounds of data collection and the use of player feedback after “execution” to label examples. However, the key difference is that in Kojima et al. (2021) the agent is a single ML model, whereas in this work, we aim to show that credit can be assigned to different components in a modular system, the data for the component can be annotated, and the component re-trained without any engineer intervention.

There are several works showing how humans can interactively teach robotic agents, for example Saxena et al. (2014); Paxton et al. (2017); Mandlekar et al. (2018); Cabi et al. (2019); Mandlekar et al. (2020). In Saxena et al. (2014), the authors demonstrate large-scale crowd-sourcing of data for perceptual and knowledge-base components of a robotics system. In Mandlekar et al. (2018; 2020) crowd-workers are connected with robotic manipulators to demonstrate movements or parts of movements. COSTAR Paxton et al. (2017) is a modular system for teaching robots to carry out tasks using behavior trees. Our work is similar to COSTAR in that it is built on a modular system with perception decoupled from action generation; but in this work we focus on the infrastructure for crowd-sourcing annotations, rather than mechanisms for live human teaching.

Finally, our work builds on the ideas of Carlson et al. (2010); Mitchell et al. (2018). Our hope is to demonstrate progress towards *embodied* incarnations of these. We show that the system is able to improve even when the module being supervised is far from the end-to-end experience the agent receives, and that architecture-naive crowd-workers operating as group can route errors to appropriate modules and teach them at scale.

4 RESULTS

4.1 NLU ERROR COLLECTION

In Table 1 the results of the NLU error generation funnel are reported. In total, over the course of the experiments, we collected 18, 163 de-duplicated commands.

In early runs, we found that training only on new data where the NLU model failed led to feedback effects. We updated our protocol to re-train using *all* de-duplicated commands at each iteration (including the ones the model correctly parsed). We leave methods for balancing the cost of labeling against distributional stability for future work.

Even though we annotated all of the commands on later re-deployments, we calculated the accuracies of workers in routing errors - in ongoing and future work we expect to have several active ML models across different modules of the agent. Workers are relatively precise: 89% of the time they mark a command as resulting in an NLU error, it turns out to be a true error. However, we estimate only 43% of NLU errors are marked. This is an estimate because it can only be calculated for commands for which there has ever been an annotation. Future work on interaction task design will attempt to address this discrepancy.

4.2 VISION MODULE ERROR COLLECTION

We started to collect vision module errors from 11_{th} iteration. After NLU module demonstrated promising results in this setting in the first 10 iterations, we integrated vision modality in to demonstrate heterogeneous learning capabilities. Over the course of following 12 iterations, we collected 695 marked vision errors, and 469 of them are successfully annotated and added to the initial dataset of size 1538.

4.3 NLU & VISION MODEL IMPROVEMENTS

For NLU models, We ran 22 iterations of the full interaction → routing → annotation → retrain pipeline. The first 5 iterations were run over a period of 3 weeks. In these, we did not re-deploy the NLU model after an iteration. For the next 18 iterations, we redeployed the re-trained model over each iteration.

Pipeline Stage	Number of Commands
All Commands	22,685
De-duplicated, Valid Commands	18,163
Marked Agent Errors	7,461
Marked NLU Errors	2,559
Marked NLU Errors Successfully Annotated	2,403
Marked "True" NLU Errors	2,138
<i>All Known NLU Errors</i>	<i>4,944</i>

Table 1: The number of commands for which each row description applies. "All Commands" refers to all commands from the data presented here. "De-duplicated, Valid Commands" refers to the subset of 'All Commands' that are unique and ask the agent to perform a task within its capabilities. "Marked Agent Errors" refers to the number of times a worker indicated, after issuing a command and observing the resulting agent behavior, that the agent failed to perform the task. "Marked NLU Errors" refers to the subset of 'Marked Agent Errors' for which workers indicated the agent did not understand the command, based on a report of the NSP output. "Marked NLU Errors Successfully Annotated" refers to the subset of 'Marked NLU Errors' for which a ground truth logical form was successfully added to the data set through the annotation process. The remainder were outstanding at the time of model retraining and redeployment but remain accessible for later use. "Marked 'True' NLU Errors" refers to the subset of 'Marked NLU Errors Successfully Annotated' for which the ground truth annotation varied from the NSP inference. The ratio of the two previous values forms the worker error marking precision. "All Known NLU Errors" refers to the subset of 'De-duplicated, Valid Commands' for which a) a ground truth logical form exists in the data set and b) the ground truth annotation varied from the NSP inference. The ratio of 'Marked "True" NLU Errors' to 'All Known NLU Errors' forms the estimate of worker error marking recall.

For vision models, the same baseline model is deployed for the first 10 iterations. Then we started to collect vision errors, annotate errors, retrain and re-deploy vision models starting from 11th iteration.

In order to measure model improvements, for each new tranche of data from the iterations, we randomly split it into a train, valid and test set. We then build a sequence of training data sets R_n which are the union of the first n training sets, V_n which are the union of the first n validation sets, and T_n , the union of the first n test sets. For NLU module, R_0 is taken from [Srinet et al. \(2020\)](#) and for vision module, R_0 is templated data we generated using rule-based scripts (see more details in Appendix). Both of them are used to train the initial deployed NLU & vision model, respectively.

For each tranche of data n , we compare three models. The first is the baseline, trained on R_0 . The next is the episode-updated model, trained on R_n (trained the same way as the model that was used for obtaining R_{n+1}). Finally, we take the episode-updated model trained on R_n , and then finetune it on R_0 ; we call this the "re-biased" model.

We repeated the model training 5 times for each tranche with different random seeds. Our main results are Figure 4, 5, 6, 7. The colored lines represent mean values of model accuracy across all 5 experiments and the shaded error bands represent the standard error.

In Figure 4, we show the performance of models trained on R_n (all the data up to the n_{th} iteration) vs. the original baseline, all tested on the final test data T_{22} (the union of the test sets from all tranches). The x axis is the total number of training examples used for that model, arranged in the sequence they were obtained, and the y axis is model performance. We can see a steady improvement on the final test set in the episode-updated models over the baseline. The re-biased model also improves, although not quite as much.

In Figure 5, we show the performance of baseline model trained on R_0 and tested on T_n (the union of the test sets over tranches). We can see a steady performance decay on the test set of each tranche in the baseline model, indicating that the tasks are getting harder over episodes, i.e. unseen data points are added to the dataset continually.

In Figure 6, we show the performance of models trained on R_n (all the data up to the n_{th} iteration) and the performance of the baseline model trained on R_0 , both tested on T_n (the union of the test sets over tranches). We can see that models trained on R_n outperform the baseline model consistently because these episode-updated models are trained with additional data points whose distribution is closer to the new data points in test set while baseline model is trained with only initial training dataset.

In Figure 7, we show the performance of models trained on R_n and testing on T_0 (the initial test data). The episode-updated models perform worse on T_0 even though they are trained with a larger amount of data; but this is not surprising, as the collection procedure for the base data R_0 was different than R_i for $i > 0$, and hence the distribution

is different. Specifically, for NLU module, most of the commands in R_0 were collected by asking crowd-workers what they might ask an agent to do offline (no interaction with the agent) and for vision module, all the objects in R_0 were generated using rule-based scripts; whereas in this work, the crowd workers are actually connected to the agent in a session, and interact with it, giving multiple commands in each session and able to create/destroy/modify objects in the world freely.

The re-biased model manages to keep its performance almost at the level of the baseline (while improving on the new data). Thus model re-biasing can mitigate the performance degradation on the original data caused by the distribution difference between newly collected data and original data, while still improving on the baseline on new data.

4.4 ANNOTATOR EXPERIENCE IMPROVEMENTS

The NLU model improvement rate is a function of the quantity and diversity of the NLU system errors, and is constrained to the first order by the resources available to fund interactions with the agent. Therefore, the goal of our UI/UX (user interface and user experience) research is to efficiently generate and correctly mark as many high quality errors as possible in each interaction, and a focus on interface usability is critical to this end. We have been guided by standard usability heuristics, the most impactful of which are listed here below.

- **Aligning With Design Standards** - Utilizing UI components and affordances that match user expectations, as well as reducing overall visual clutter helps reduce cognitive load of using the interface.
- **Forced Choices** - Providing clear, blocking choices for important UI tasks rather than relying on the user to recognize a branch in workflow and select the appropriate option.
- **Visual Feedback** - Implementing clear and easy to understand visual indicators of agent status as well as the quality of the interaction (number and diversity of commands) helps the workers understand our expectations better.
- **Performance Incentives** - Shifting to paying workers a lower base rate with incentives for good performance both: lowers the cost of data collection on a per-error basis and results in higher worker pay.

While there is not an obvious baseline of usability for a specific interface, Figure 9 shows the cost efficiency improvements for each iteration as the project progressed, providing a strong validation of effort spent improving task usability. Over the course of the four UI/UX experiments listed, the cost of collecting a single NLU error fell by 71%. Below is more detail on the nature of each of the four UI/UX experiments. The experiments are cumulative, meaning each experiment includes the changes made in the previous.

4.4.1 EXPERIMENT 1 - CLARITY AND VERBOSITY

The goal of the first experiment was to reduce visual clutter, verbosity, and text complexity. Hirth et al. (2020) finds that "Incomprehensible Instructions" are the single most frustrating aspect of task design when present. Experiment 1 reduced the number of instruction words by almost half, and paginated the remaining so workers were never reading more than a few sentences at a time. The instructions are attached in Appendix B, Figure 14. After the initial read during the task, instructions are hidden but available through a drop-down mechanism to further reduce clutter on screen. The information from the instructions most relevant to producing good interaction data is copied outside the instructions window immediately next to the interaction interface for easy reference.

4.4.2 EXPERIMENT 2 - VISUAL FEEDBACK AND FORCED CHOICES

The purpose of the second experiment was to ensure that the worker is not confused about the agent status or what to do next. After each command, the agent must receive and interpret it, then potentially plan and carry out an action or set of actions, as well as respond to the user if appropriate. Experiment 2 introduced messages to report the agent status periodically.

The second change in this experiment was to make the error marking decision tree described in Section 2.4.2 and shown in Figures 17 and 18 in the Appendix. If error marking is a passive call-to-action, workers may not mark effectively because they may not remember to mark erroneous commands or may be eager to move on with the task. By forcing the worker to decide one way or the other before continuing, a much higher percentage of agent errors are captured.

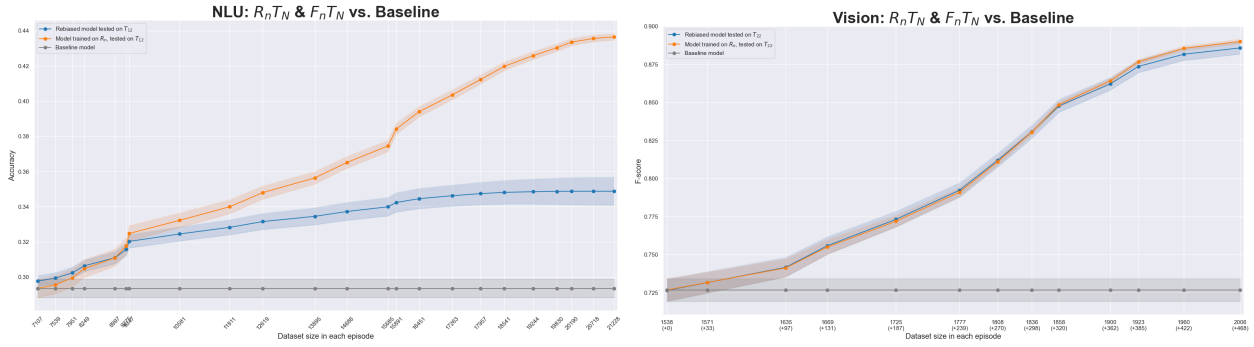


Figure 4: Episode-updated model tested on T_{all} (union of all collected test data). We can see a steady improvement on the final test set in the episode-updated models over the baseline model. Orange is continually learned, Blue is re-biased, and Gray is baseline.

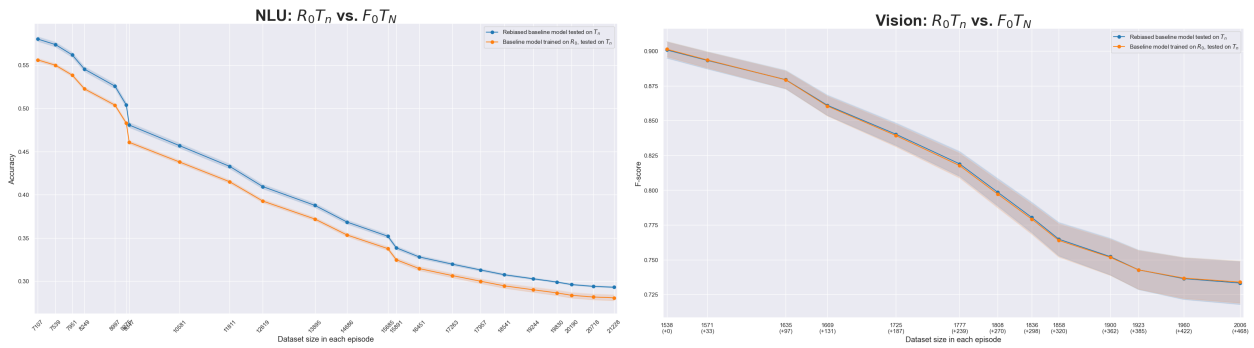


Figure 5: Baseline model tested on T_n (union of test data over tranches). The performance decay indicates the tasks become harder over tranches (i.e. unseen data points are added to dataset continually)

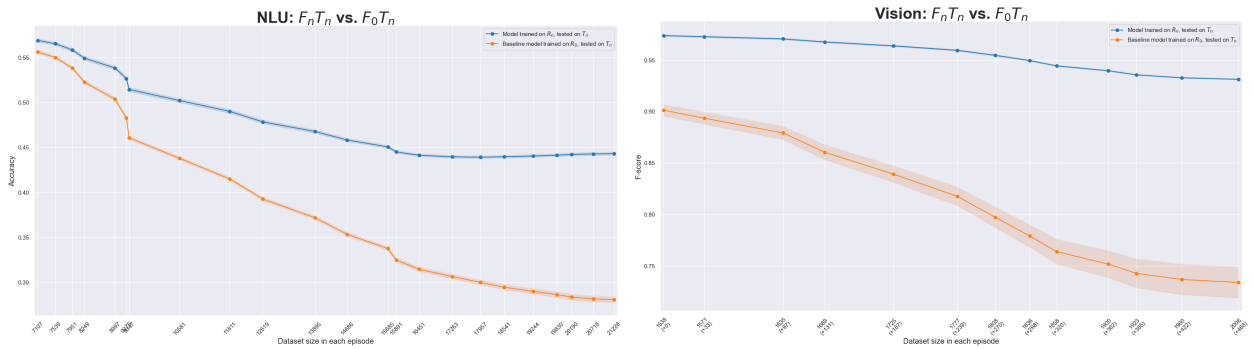


Figure 6: Episode-updated model tested on T_n (union of test data over tranches) vs. Baseline model performance tested on T_n . Episode-update models outperform baseline models consistently over each tranche.

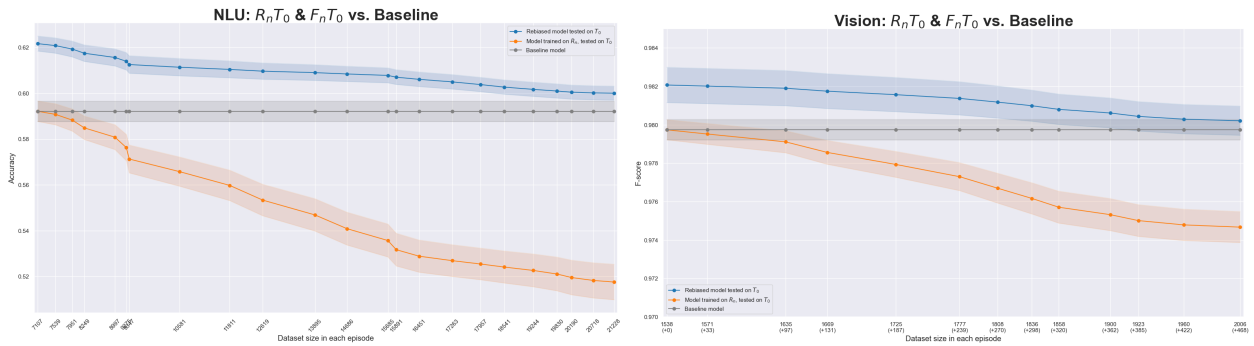


Figure 7: Episode-updated model (Orange) tested on T_0 (the initial test data). Distribution shift caused the performance decay, and model re-biasing (Blue) mitigated this problem with some performance improvement over baseline (Gray).

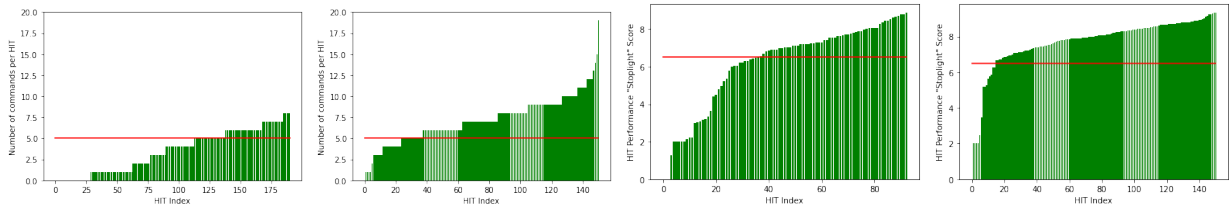


Figure 8: The charts above show the number of commands workers issued per interaction task (left two charts) and the stoplight performance score described in Section 4.4.3 (right two charts) before (first and third charts) and after (second and fourth charts) issuing performance incentives. The red line indicates the authors’ target for each metric. There are fewer data in the third chart, because a recording bug in UI/UX Experiment 3 caused half of these data to be lost.

Experiment Name	Number of tasks Completed	Data Generation Efficiency Ratio
Baseline	17	1.0
Exp1 - Instruction Clarity and Verbosity	106	1.1
Exp2 - Visual Feedback and Forced Choices	197	2.5
Exp3 - Design Standards Alignment	191	3.1
Exp4 - Performance Incentives	150	3.5

Figure 9: Table showing the the efficiency of data collection (NLU errors collected per \$) as I/UX improvements were made, reported as a ratio between the efficiency of that experiment and the baseline value before any UI/UX improvements were made. Data generation efficiency is computed as an average over all tasks completed in that experiment. UI/UX experiments are cumulative, not independent (each includes the changes of the previous).

4.4.3 EXPERIMENT 3 - ALIGN WITH DESIGN STANDARDS

Human-Computer Interaction research has shown that familiarity with an interface reduces cognitive load, and therefore increases task accuracy and reduces task completion time. For a review of this concept see [Hollender et al. \(2010\)](#). Experiment 3 replaced the chat interface with a UI that closely resembles that one would find on a cell phone or the help window of a website, with the purposes of better aligning with workers’ existing mental model of a chat interface.

This experiment also introduced a new component to the interface - a stoplight that serves as a feedback indicator of the overall task performance to the worker. If the light is red the worker knows that their performance is unsatisfactory, and so forth. The metric used to determine the stoplight color is a weighted average of the log of: the number of commands issued, the diversity of commands in-session (average word edit distance between each session command), and the average creativity of the commands (word edit distance compared to all previously issued commands). The weights and thresholds driving the stoplight indicator were empirically tuned to align with the results a worker should obtain by engaging in good faith with the task.

4.4.4 EXPERIMENT 4 - PERFORMANCE INCENTIVES

The final experiment in this series was meant to operationalize the stoplight introduced in the previous section by offering performance incentives based on the “stoplight score”, or the score out of 10 that determines the stoplight color. In this experiment, workers receive a lower base pay in addition to a bonus payment after completion based on their score. Workers can see their expected bonus reported in real time after they issue each command.

This change had several notable effects. Firstly, nearly all of the workers achieved a score in the “green” performance band, compared to the previous experiment where approximately 2/3 did, shown in Figure 8. Second, while the cost per interaction task went up, and therefore worker compensation per time went up, data generation efficiency measured in NLU errors per dollar actually rose. Furthermore, workers responded to the change positively, providing qualitative feedback that in addition to increasing their compensation, the change also improved the enjoyability and clarity of the task. This is evidence that further task gamification and/or incentives alignment may be fruitful and mutually beneficial direction for future research.

5 DISCUSSION

In this work we have given an example of a pipelined ML powered embodied agent that uses end-to-end interaction as a crucial part of its learning mechanism; and demonstrated that the agent, and specifically the NLU module and Vision module of the agent, can improve over multiple rounds of re-deployment with human feedback in the loop. This is made possible in part through good UX allowing naive crowdworkers with no knowledge of the agent architecture to route errors and complete complex annotations in an assembly-line style.

In future work, we would like to extend the approaches discussed in this work to embodied agents with learnable Task executors; or even learnable memory and Controller modules. More generally, we think these approaches will also be valuable in the context of works like [Dalmia et al. \(2019\)](#); [Veniat et al. \(2020\)](#) that build modular ML systems that allow automatic credit assignment. The approach presented in this paper could act as a hybrid that empowers humans to teach the system at the level of its modules while automatically assigning credit when such humans are unavailable. We believe this could be more powerful than pure end-to-end or pipelined systems.

REFERENCES

- Huggingface’s transformers: State-of-the-art natural language processing. URL <https://github.com/huggingface/transformers>.
- Charles Beattie, Joel Z Leibo, Denis Teplyashin, Tom Ward, Marcus Wainwright, Heinrich Küttler, Andrew Lefrancq, Simon Green, Víctor Valdés, Amir Sadik, et al. Deepmind lab. *arXiv preprint arXiv:1612.03801*, 2016.
- Serkan Cabi, Sergio Gómez Colmenarejo, Alexander Novikov, Ksenia Konyushkova, Scott Reed, Rae Jeong, Konrad Żolna, Yusuf Aytar, David Budden, Mel Vecerik, Oleg Sushkov, David Barker, Jonathan Scholz, Misha Denil, Nando de Freitas, and Ziyu Wang. Scaling data-driven robotics with reward sketching and batch reinforcement learning. Technical report, Deepmind, 2019.
- Andrew Carlson, Justin Betteridge, Bryan Kisiel, Burr Settles, Estevam R Hruschka, and Tom M Mitchell. Toward an architecture for never-ending language learning. In *Twenty-Fourth AAAI conference on artificial intelligence*, 2010.
- Siddharth Dalmia, Abdelrahman Mohamed, Mike Lewis, Florian Metze, and Luke Zettlemoyer. Enforcing encoder-decoder modularity in sequence-to-sequence models. *arXiv preprint arXiv:1911.03782*, 2019.
- Jacob Devlin, Ming-Wei Chang, Kenton Lee, and Kristina Toutanova. Bert: Pre-training of deep bidirectional transformers for language understanding. *ArXiv*, abs/1810.04805, 2019.
- Steven Dow, Anand Kulkarni, Scott Klemmer, and Björn Hartmann. Shepherding the crowd yields better work. In *Proceedings of the ACM 2012 Conference on Computer Supported Cooperative Work, CSCW ’12*, pp. 1013–1022, New York, NY, USA, 2012. Association for Computing Machinery. ISBN 9781450310864. doi: 10.1145/2145204.2145355.
- William H Guss, Brandon Houghton, Nicholay Topin, Phillip Wang, Cayden Codel, Manuela Veloso, and Ruslan Salakhutdinov. Minerl: A large-scale dataset of minecraft demonstrations. *arXiv preprint arXiv:1907.13440*, 2019.
- Braden Hancock, Antoine Bordes, Pierre-Emmanuel Mazare, and Jason Weston. Learning from dialogue after deployment: Feed yourself, chatbot! *arXiv preprint arXiv:1901.05415*, 2019.
- Matthias Hirth, Kathrin Borchert, Katrien De Moor, Vanessa Borst, and Tobias Hoßfeld. Personal task design preferences of crowdworkers. In *2020 Twelfth International Conference on Quality of Multimedia Experience (QoMEX)*, pp. 1–6, 2020. doi: 10.1109/QoMEX48832.2020.9123094.
- Nina Hollender, Cristian Hofmann, Michael Deneke, and Bernhard Schmitz. Integrating cognitive load theory and concepts of human-computer interaction. *Computers in Human Behavior*, 26(6):1278–1288, 2010. ISSN 0747-5632. doi: <https://doi.org/10.1016/j.chb.2010.05.031>. URL <https://www.sciencedirect.com/science/article/pii/S0747563210001718>.
- Douwe Kiela, Max Bartolo, Yixin Nie, Divyansh Kaushik, Atticus Geiger, Zhengxuan Wu, Bertie Vidgen, Grusha Prasad, Amanpreet Singh, Pratik Ringshia, et al. Dynabench: Rethinking benchmarking in nlp. *arXiv preprint arXiv:2104.14337*, 2021.
- Noriyuki Kojima, Alane Suhr, and Yoav Artzi. Continual learning for grounded instruction generation by observing human following behavior. *Transactions of the Association for Computational Linguistics*, 9:1303–1319, 2021.

-
- Ajay Mandlekar, Yuke Zhu, Animesh Garg, Jonathan Booher, Max Spero, Albert Tung, Julian Gao, John Emmons, Anchit Gupta, Emre Orbay, et al. Roboturk: A crowdsourcing platform for robotic skill learning through imitation. In *Conference on Robot Learning*, pp. 879–893. PMLR, 2018.
- Ajay Mandlekar, Danfei Xu, Roberto Martín-Martín, Yuke Zhu, Li Fei-Fei, and Silvio Savarese. Human-in-the-loop imitation learning using remote teleoperation. *arXiv preprint arXiv:2012.06733*, 2020.
- Tom Mitchell, William Cohen, Estevam Hruschka, Partha Talukdar, Bishan Yang, Justin Betteridge, Andrew Carlson, Bhavana Dalvi, Matt Gardner, Bryan Kisiel, et al. Never-ending learning. *Communications of the ACM*, 61(5): 103–115, 2018.
- Chris Paxton, Andrew Hundt, Felix Jonathan, Kelleher Guerin, and Gregory D Hager. Costar: Instructing collaborative robots with behavior trees and vision. In *2017 IEEE international conference on robotics and automation (ICRA)*, pp. 564–571. IEEE, 2017.
- Aleksei Petrenko, Erik Wijmans, Brennan Shacklett, and Vladlen Koltun. Megaverse: Simulating embodied agents at one million experiences per second. In *International Conference on Machine Learning*, pp. 8556–8566. PMLR, 2021.
- Anurag Pratik, Soumith Chintala, Kavya Srinet, Dhiraj Gandhi, Rebecca Qian, Yuxuan Sun, Ryan Drew, Sara Elkafrawy, Anoushka Tiwari, Tucker Hart, et al. droidlet: modular, heterogenous, multi-modal agents. In *2021 IEEE International Conference on Robotics and Automation (ICRA)*, pp. 13716–13723. IEEE, 2021.
- Alec Radford, Jong Wook Kim, Chris Hallacy, Aditya Ramesh, Gabriel Goh, Sandhini Agarwal, Girish Sastry, Amanda Askell, Pamela Mishkin, Jack Clark, et al. Learning transferable visual models from natural language supervision. In *International Conference on Machine Learning*, pp. 8748–8763. PMLR, 2021.
- Alexander Ratner, Stephen H Bach, Henry Ehrenberg, Jason Fries, Sen Wu, and Christopher Ré. Snorkel: Rapid training data creation with weak supervision. In *Proceedings of the VLDB Endowment. International Conference on Very Large Data Bases*, volume 11, pp. 269. NIH Public Access, 2017.
- Manolis Savva, Abhishek Kadian, Oleksandr Maksymets, Yili Zhao, Erik Wijmans, Bhavana Jain, Julian Straub, Jia Liu, Vladlen Koltun, Jitendra Malik, et al. Habitat: A platform for embodied ai research. In *Proceedings of the IEEE/CVF International Conference on Computer Vision*, pp. 9339–9347, 2019.
- Ashutosh Saxena, Ashesh Jain, Ozan Sener, Aditya Jami, Dipendra K Misra, and Hema S Koppula. Robobrain: Large-scale knowledge engine for robots. *arXiv preprint arXiv:1412.0691*, 2014.
- Rohin Shah, Cody Wild, Steven H Wang, Neel Alex, Brandon Houghton, William Guss, Sharada Mohanty, Anssi Kanervisto, Stephanie Milani, Nicholay Topin, et al. The minerl basalt competition on learning from human feedback. *arXiv preprint arXiv:2107.01969*, 2021.
- Kurt Shuster, Jack Urbanek, Emily Dinan, Arthur Szlam, and Jason Weston. Dialogue in the wild: Learning from a deployed role-playing game with humans and bots. In *Findings of the Association for Computational Linguistics: ACL-IJCNLP 2021*, pp. 611–624, 2021.
- Patrice Y Simard, Saleema Amershi, David M Chickering, Alicia Edelman Pelton, Soroush Ghorashi, Christopher Meek, Gonzalo Ramos, Jina Suh, Johan Verwey, Mo Wang, et al. Machine teaching: A new paradigm for building machine learning systems. *arXiv preprint arXiv:1707.06742*, 2017.
- Kavya Srinet, Yacine Jernite, Jonathan Gray, and Arthur Szlam. Craftassist instruction parsing: Semantic parsing for a voxel-world assistant. In *Proceedings of the 58th Annual Meeting of the Association for Computational Linguistics*, pp. 4693–4714, 2020.
- Alane Suhr, Claudia Yan, Jacob Schluger, Stanley Yu, Hadi Khader, Marwa Mouallem, Iris Zhang, and Yoav Artzi. Executing instructions in situated collaborative interactions. *arXiv preprint arXiv:1910.03655*, 2019.
- Tom Veniat, Ludovic Denoyer, and Marc’Aurelio Ranzato. Efficient continual learning with modular networks and task-driven priors. *arXiv preprint arXiv:2012.12631*, 2020.
- Sida I Wang, Samuel Ginn, Percy Liang, and Christopher D Manning. Naturalizing a programming language via interactive learning. *arXiv preprint arXiv:1704.06956*, 2017.
- Xingjiao Wu, Luwei Xiao, Yixuan Sun, Junhang Zhang, Tianlong Ma, and Liang He. A survey of human-in-the-loop for machine learning. *arXiv preprint arXiv:2108.00941*, 2021.

A AGENT'S DOMAIN SPECIFIC LANGUAGE(DSL)

This section describes the details of logical form of each action pictorially. We support three dialogue types: HUMAN_GIVE_COMMAND, GET_MEMORY and PUT_MEMORY. We support the following actions in our dataset : Build, Dance, Get, Spawn, Resume, Fill, Destroy, Move, Undo, Stop, Dig and FreeBuild.

In figure 10, we represent an event in the agent's grammar and DSL:

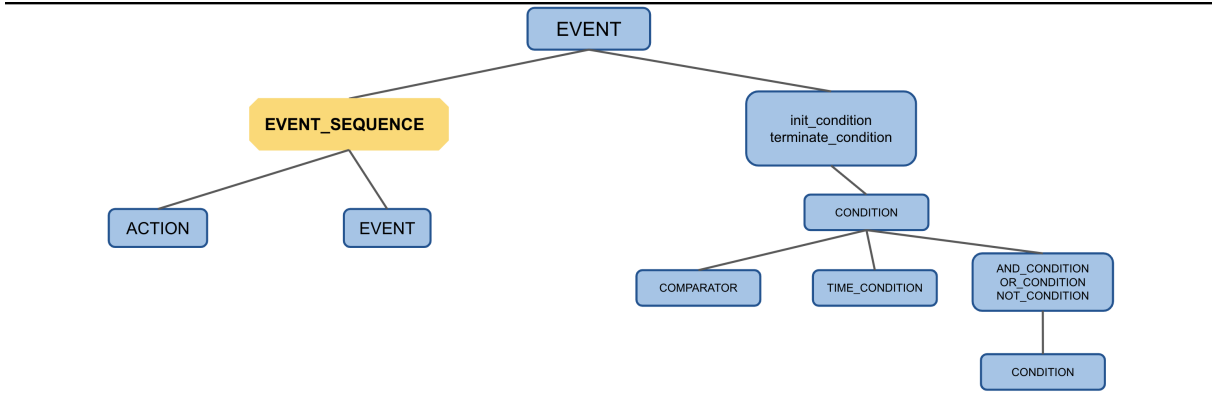


Figure 10: The agent's DSL showing the structure of an event.

In figure 11, we show a full pictorial representation of actions in the agent's DSL:

Filters add a lot of expressiveness to the agent's grammar, we show a representation of filters in figure 12

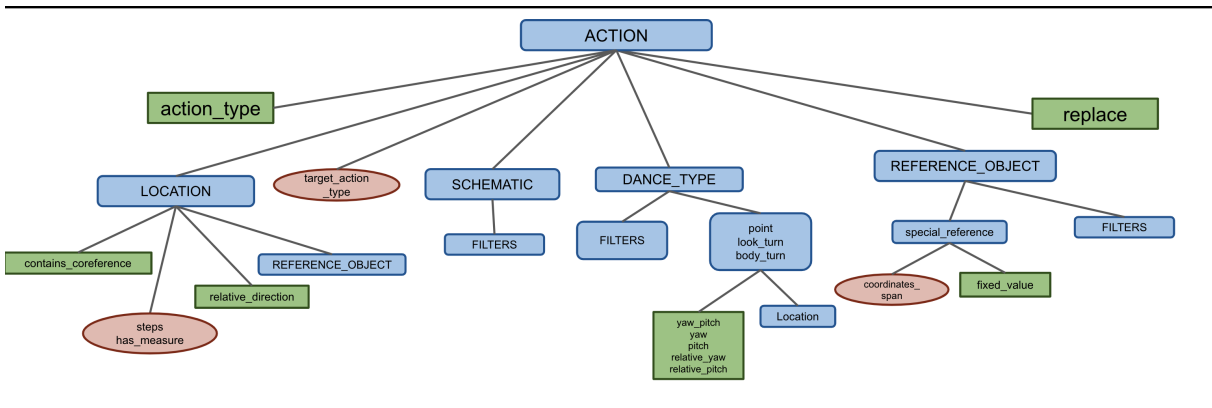


Figure 11: The representation of an action in agent's DSL.

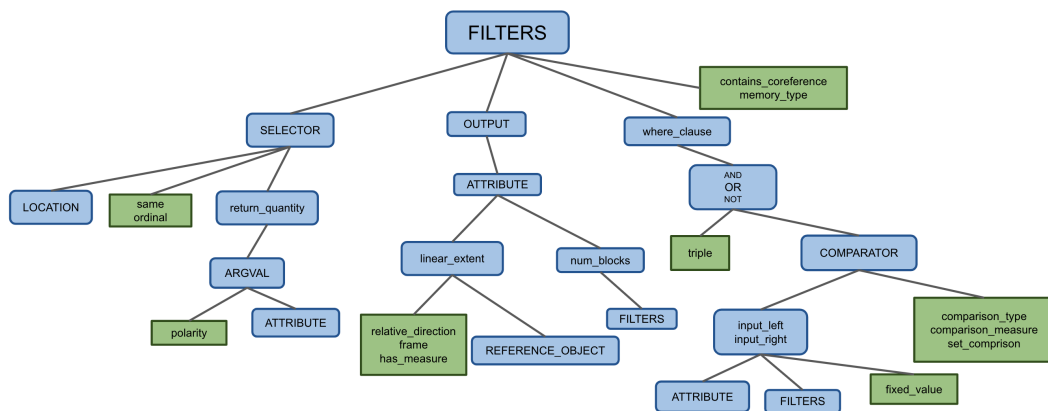


Figure 12: The representation of filters in agent's DSL.

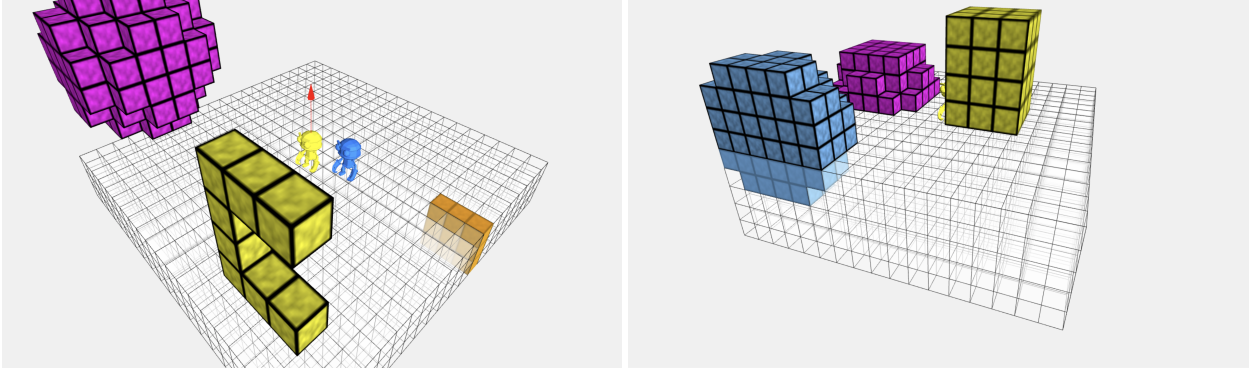


Figure 13: Examples of templated vision data generated using rule-based scripts, rendered in our 3D visualization tool

B VISION MODULE DETAILS

B.1 VISION MODEL ARCHITECTURE

This section describes the details of vision model architecture. The vision model consists of a Voxel Encoder to extract visual features and a Text Encoder to extract text features.

Voxel Encoder is 4-layer 3D convolutional neural network trained from scratch. For each layer, it consists of a 3D convolutional module with $kernel_size = 5$, $hidden_dim = 128$ and $padding = 2$, followed by a 3D Batch Normalization module and a ReLU activation function to extract visual features $F_V \in \mathbb{R}^{H \times W \times L \times C}$ (H denotes height, W denotes width, L denotes length and C denotes hidden dimension).

Text Encoder For any text input $T \in \mathbb{R}^L$, we directly use a frozen CLIP [Radford et al. \(2021\)](#) Text Encoder to extract text features $F_T \in \mathbb{R}^{C \times L}$, where $c = 768$. Then we use a projection layer which transforms the $hidden_dim$ from 768 to 128 to match the hidden dimension of Voxel Encoder output.

Once we got both visual features $F_V \in \mathbb{R}^{H \times W \times L \times C}$ and text features $F_T \in \mathbb{R}^{C \times L}$, we perform matrix-matrix product on them followed by a *sigmoid* layer to generate voxel-wise probability distribution $P \in \mathbb{R}^{H \times W \times L}$ on how likely each voxel belongs to the object referred in the text. All voxels with probability high than $threshold = 0.8$ are then used to construct the segmentation mask as model output.

B.2 VISION DATA BOOTSTRAPPING

This section describes how we use rule-based scripts to generate initial training data which we use to train vision baseline models.

We randomly put 1 to 3 shape objects with different materials and sizes into the 3D flat voxel world [2.1.1](#) and record the world state (i.e. voxel IDs at each voxel position) as schematics. The shape object is created purely based on mathematical formulas. For example, the schematic of a solid sphere with center (x, y, z) and radius r consists of all the points (ix, iy, iz) in the space, where $(\sqrt{(ix-x)^2 + (iy-y)^2 + (iz-z)^2}) \leq r$. [Figure 13](#) shows two examples of data points generated in this way, rendered in our 3D visualization tool.

The full list of shapes that we used is as follows: cube, rectanguloid, sphere, pyramid, square, rectangle, circle, triangle, dome, arch. We construct the text description of these shapes based on their names and colors (since it’s rule based, we have prior knowledge of the material of each voxel and the color of it). For example, a cube made of gold blocks could be named as ‘cube’, ‘yellow cube’ or ‘the yellow thing’ randomly.

Furthermore, we construct some negative data points based on the positive ones, that is, we randomly ask objects that are not in the generated scenes. The segmentation masks of those non-existing objects are all empty.

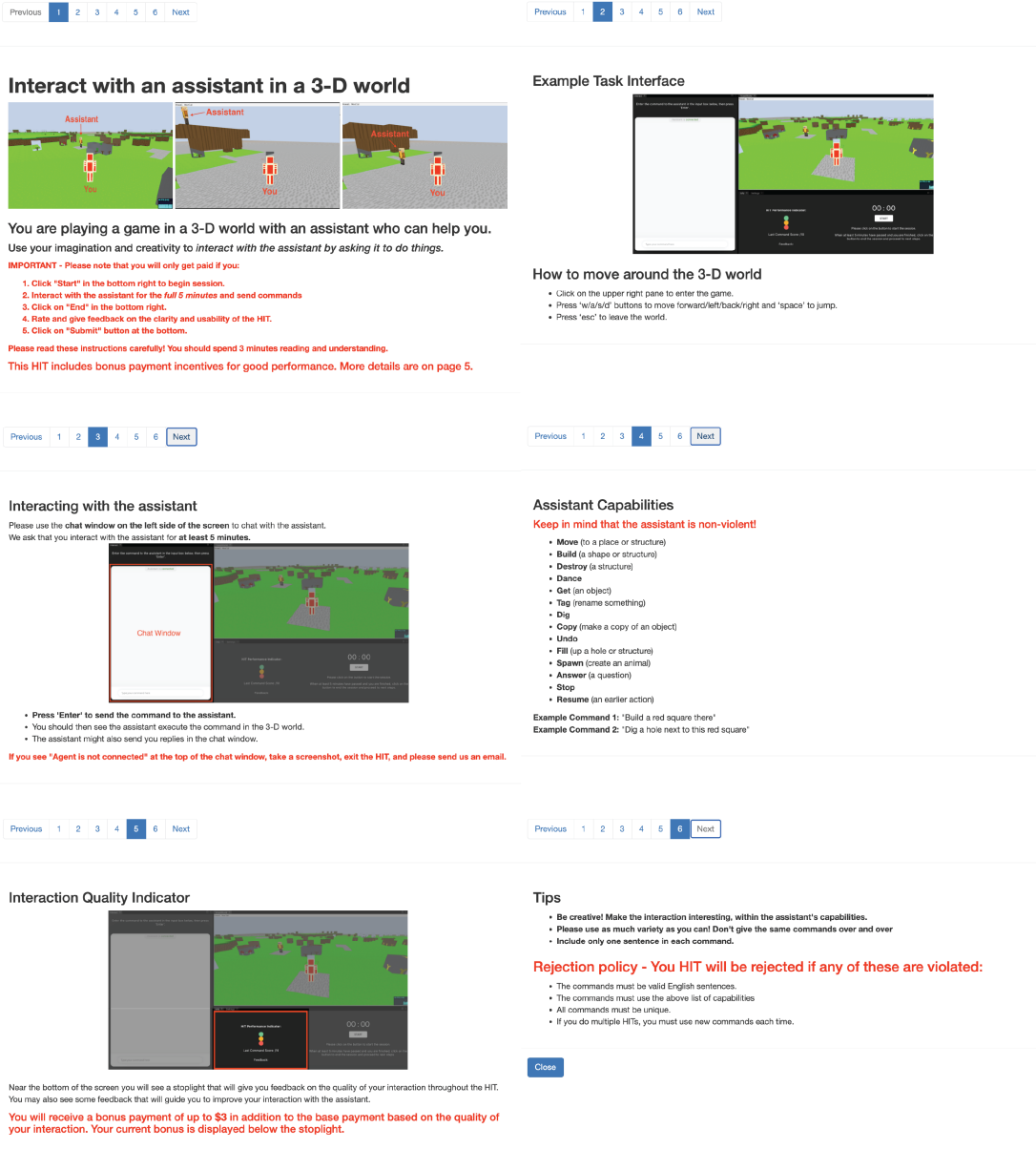


Figure 14: The instructions given to crowd-sourced workers for completing the agent interaction HIT.

C DATA GENERATION INTERFACE - HUMAN INTELLIGENCE TASK (HIT)

This appendix describes the interface used by crowd-sourced workers to interact with the Droidlet agent and generate data by issuing commands.

Figure 14 is the instructions popup, which is the first thing that the worker sees when starting the HIT. The instructions are paginated to reduce each section to a digestible amount of content.

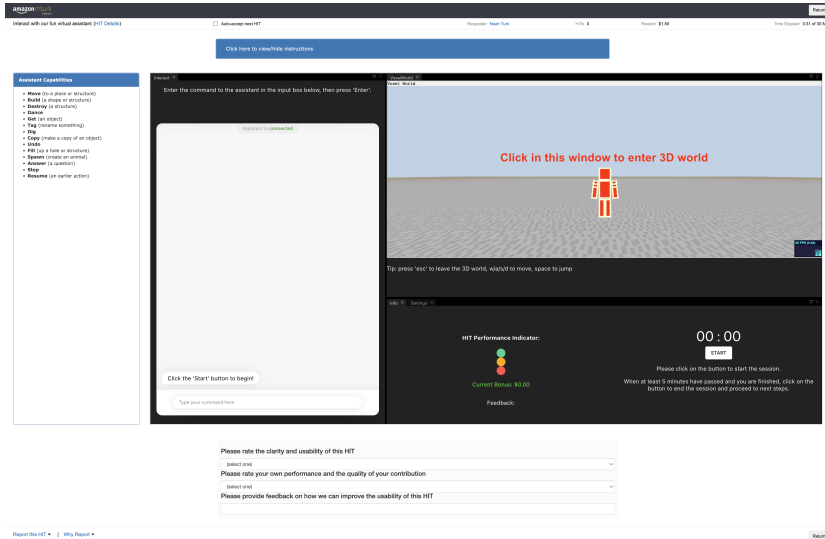


Figure 15: View of the HIT page at the beginning of the task.

Figure 15 shows the view of the HIT page that workers see at the beginning of the task. There is a prompt in the chat to start the clock (each interaction is a minimum of five minutes), and there is a prompt superimposed over the voxel world window indicating that users need to click once in that window in order for the voxel world to render. The "stoplight" performance score is a 0 out of 10 at the start of the HIT, and no feedback is available yet. The instructions, which were shown in a popup previously, are available for review in the dropdown at the top of the page. However, the agent capabilities are always available for easy reference just to the left of the interaction window.

Figure 16 shows two of the status messages that workers see after submitting a command. These status messages are available so that the worker is not confused about what is happening at any given time, and can more reliably identify if there is a bug or the agent has frozen. The four status messages that are shown after every command are, in order: "sending command", "command received", "assistant thinking", and "assistant is doing the task". The first is cleared when the agent acknowledges having received the command. The second is cleared after 500ms. The third is cleared after the NSP has parsed the command. The fourth and final status is cleared after the agent has completed the task, if it knows how. After the fourth status message is cleared the next UI screen that appears is the error routing screen, which the user must progress through before being allowed to issue another command.

Figure 17 and Figure 18 show the error marking flows after the agent processes a command containing an NLU error and a non-NLU task error, respectively. Correct error marking is critical in order to appropriately route the appropriate data to the appropriate annotator. After completing this decision tree presented one question at a time, the worker is returned back to the original interaction window shown in Figure 1.



Figure 16: Status update messages given to workers as the agent is processing instructions and performing the task. The worker retains the ability to issue a "stop" command while the agent is working.

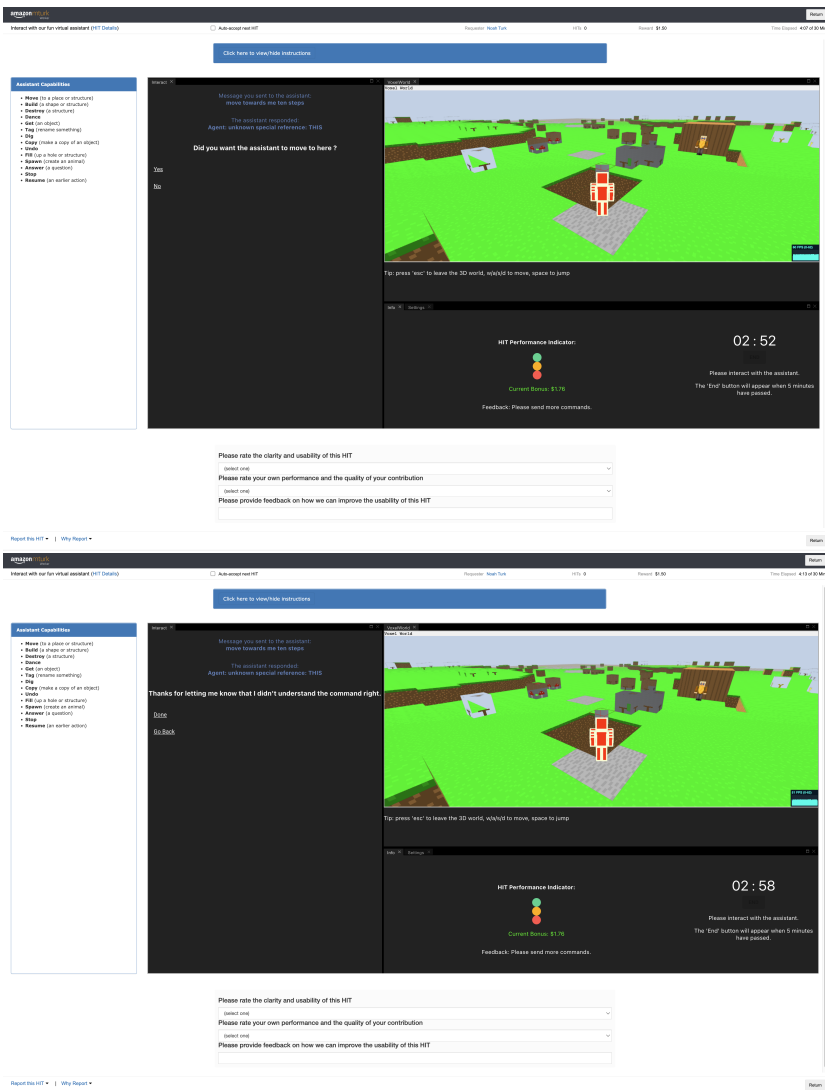


Figure 17: Error routing flow for a command that contains an NLU error.

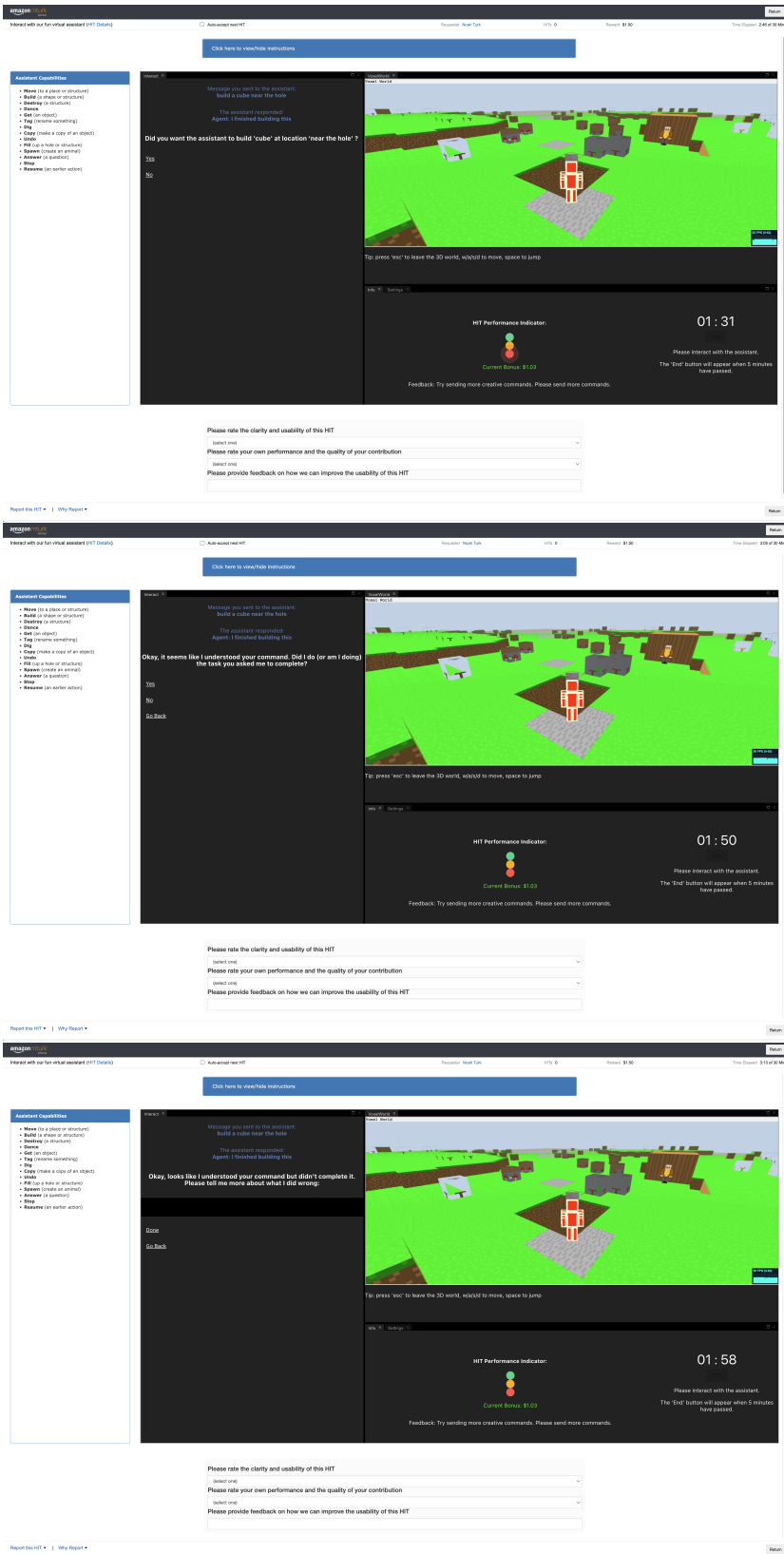


Figure 18: Error routing flow for a command that does not contain an NLU error but which the agent does not complete correctly (in this case a perception error).

D VISION ANNOTATION TOOL DETAILS

This section describes the details of vision annotation tool which crowdsourced workers used to annotate vision errors. For each object our vision model failed to recognize in a given scene, we extract the text description of that object and a snapshot of the 3D voxel world state and re-render in this web-based vision annotation tool. Crowdsourced workers are then asked to mark the blocks corresponding with the object as shown in figure 19.

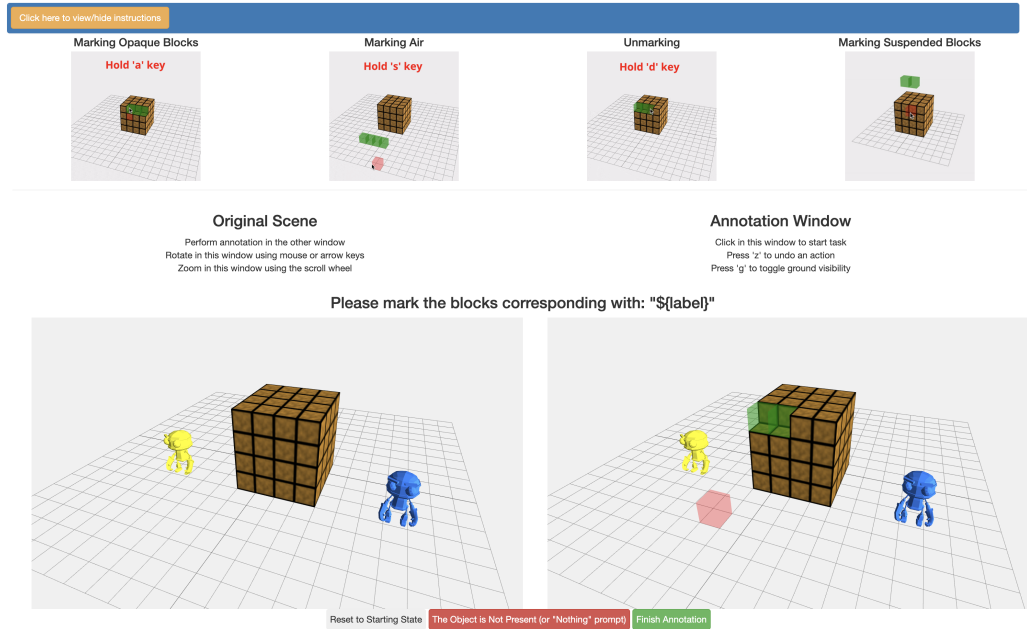


Figure 19: Vision annotation tool

Full instructions of how to use this tool are shown in figure 20.

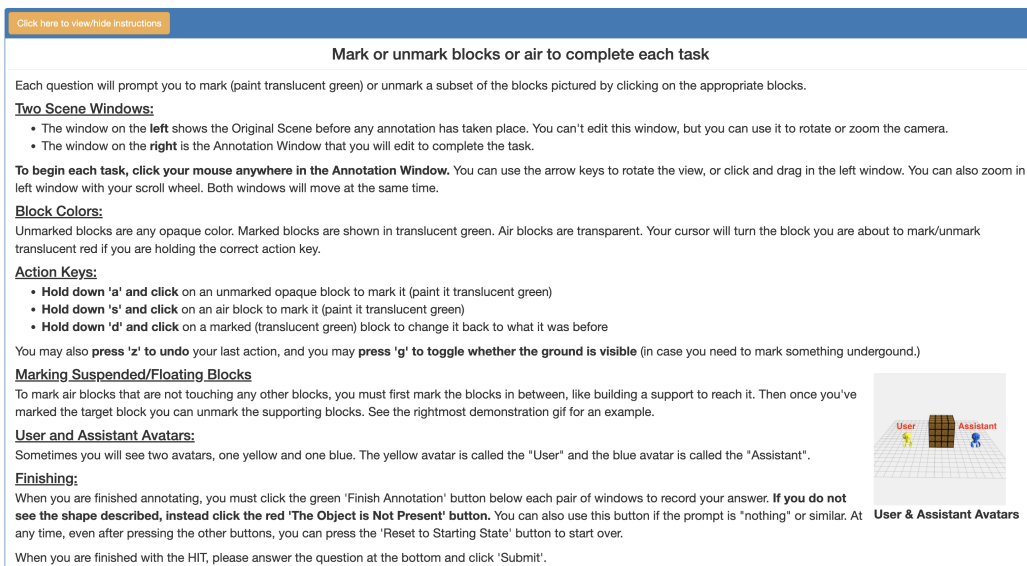


Figure 20: Vision annotation tool instructions

E MODEL TRAINING DETAILS

E.1 NLU MODULE

For the standard model retraining job, we train the models for 100 epochs (on average till lack of improvement on V_n). The batch size is set to 24 in order to fit into a single 16G GPU chip.

For Transformer decoder learning rate, we are choosing between 0.0000005, 0.000001 and 0.000005 while for the encoder learning rate we are choosing between 0.0 and 0.000001. This gives us a total number of 6 different combinations of hyperparameters for each model training job; we validate on V_n . All other parameters are the default from [hug](#).

For model re-biasing, we train the models on the original training dataset for 10 epochs (this is roughly till lack of improvement on V_0 , the initial validation set from [Srinet et al. \(2020\)](#)).

E.2 VISION MODULE

For the standard model retraining job, we train the models for 4000 epochs (on average till lack of improvement on V_n). For model re-biasing, we train the models on the original training dataset for 50 epochs (this is roughly till lack of improvement on V_0 , the initial validation set we generated using rule-based python scripts).

For hyperparameter search, we are choosing between 128 and 256 for voxel encoder hidden dimension size. For learning rate we are choosing between 0.001 and 0.0001. For probability threshold of being classified as positive we are choosing between 0.3, 0.5 and 0.8. This gives us a total number of 12 different combination. We trained the baseline vision models with those hyperparameters and this combination (hidden_dim=128, learning_rate=0.001, probability_threshold=0.8) outperformed other combinations greatly, so we use this specific hyperparameter set for all the training jobs in the following iterations.